A synergistic relationship between three regions of stathmin family proteins is required for the formation of a stable complex with tubulin

Isabelle JOURDAIN*, Sylvie LACHKAR*, Elodie CHARBAUT*, Benoit GIGANT†, Marcel KNOSSOW†, André SOBEL* and Patrick A. CURMI*[1]

*Signalisation et Différenciation Cellulaires dans les Systèmes Nerveux et Musculaire, U440 Institut National de la Santé et de la Recherche Médicale/Université Pierre et Marie Curie, Institut du Fer à Moulin, 17 rue du Fer à Moulin, 75005 Paris, France, and †LEBS, UPR 9063, Centre National de la Recherche Scientifique, Gif-sur-Yvette, France

Stathmin is a ubiquitous 17 kDa cytosolic phosphoprotein proposed to play a general role in the integration and relay of intracellular signalling pathways. It is believed to regulate microtubule dynamics by sequestering tubulin in a complex made of two tubulin heterodimers per stathmin molecule (T_2S complex). The other proteins of the stathmin family can also bind two tubulin heterodimers through their SLD (stathmin-like domain), but the different tubulin:SLD complexes display varying stabilities. In this study, we analysed the relative influence of three regions of SLDs on the interaction with tubulin and the mechanistic processes that lead to its sequestration. Tubulin-binding properties of fragments and chimaeras of stathmin and $RB3_{SLD}$ were studied *in vitro* by tubulin polymerization, size-exclusion chromatography and surface plasmon resonance assays. Our results show that the N-terminal region of SLDs favours the binding of the first tubulin heterodimer and that the second C-terminal tubulin-binding site confers the specific stability of a given tubulin:SLD complex. Our results highlight the molecular processes by which tubulin co-operatively interacts with the SLDs. This knowledge may contribute to drug development aimed at disturbing microtubules that could be used for the treatment of cancer.

Key words: microtubule, RB3 (rat brain-3), stathmin, tubulin.

INTRODUCTION

Microtubules are polymers made of α/β tubulin heterodimers that assemble and disassemble in a closely regulated dynamic manner. They are major components of the cytoskeleton involved in numerous cellular functions such as mitosis, cell motility or location of membrane-bound organelles. A characterization of microtubule regulations is thus of importance for the understanding of cell function under normal and pathological conditions.

Stathmin [1], also named Op18 [2], is a ubiquitous cytosolic protein that participates in the control of microtubule dynamics [3]. It prevents tubulin polymerization or promotes microtubule disassembly in a phosphorylation-dependent manner [4–7]. As it can be differently phosphorylated in response to hormones [8], growth factors [9] or neurotransmitters [10], stathmin is thought to integrate diverse intracellular signalling pathways [11] that may interfere with various microtubule-dependent cellular functions [12,13]. Moreover, stathmin is overexpressed in many types of cancers [14–17], where these regulations are altered, an abnormality that may be exploited for new therapeutic approaches. It has been demonstrated that stathmin can sequester free tubulin in a non-polymerizable ternary complex made of one stathmin molecule and two α/β tubulin heterodimers (T_2S complex) [18–22]. This mechanism accounts for most of the reported stathmin activities regarding microtubules. Alternatively, it has been proposed that stathmin could have other effects on tubulin and microtubules, such as direct interaction with microtubule ends or promotion of the tubulin GTPase activity [3,23,24].

Stathmin is the generic element of a protein family, including SCG10 (superior cervical ganglia protein 10), SCLIP (SCG10-like protein) and RB3 (rat brain-3), that share a highly conserved SLD (stathmin-like domain) [25–28]. From a functional point of view, all SLDs are able to sequester tubulin in a T_2S complex. The crystallographic resolution of the $RB3_{SLD}$:tubulin complex [21], with the electron micrographs of the tubulin:stathmin complex [20], shows that the general organization of these two complexes is very similar, suggesting that the SLDs sequester tubulin according to the same mechanism. However, the complexes so formed display very different stabilities [28], the T_2S complex formed with $RB3_{SLD}$ being, for example, much more stable than that formed with stathmin. Such diversity needs to be studied to understand its physiological and functional relevance.

The X-ray structure of the tubulin:$RB3_{SLD}$ complex [21] shows that it is made of two tubulin heterodimers aligned head-to-tail ($\alpha\beta$–$\alpha\beta$) centred on a 91-residue SLD α-helix. The limits of the SLD α-helix were not determined but secondary-structure algorithms predict an α-helix covering approx. 90 residues. This predicted α-helix contains an internal tandem repeat (40 % sequence identity, 74 % similarity for stathmin) [21,29], which suggests that each copy of the repeat probably faces one α/β tubulin heterodimer. Furthermore, cross-linking experiments [30] and recent X-ray crystallographic studies (R. B. G. Ravelli, B. Gigant, P. A. Curmi, I. Jourdain, S. Lachkar, A. Sobel and M. Knossow, unpublished work) revealed that the region N-terminal to the α-helix interacts with α-tubulin. Considering the head-to-tail arrangement of the tubulin heterodimers in the complex, this finding indicates that the N-terminal region caps the edging α-tubulin monomer of the T_2S complex. Overall, these results provide a picture of the tubulin:SLD complex structure (Figure 1). However, the mechanisms that lead to the formation and stabilization of the complex and that make each SLD unique regarding tubulin sequestration still remain undescribed.

In the present study, we measured the relative contribution of the N-terminal region, the first and second tubulin-binding sites

Abbreviations used: DTT, dithiothreitol; RU, resonance unit; SLD, stathmin-like domain; SPR, surface plasmon resonance; TMAO, trimethylamine-*N*-oxide.

[1] To whom correspondence should be addressed (e-mail curmi@fer-a-moulin.inserm.fr).

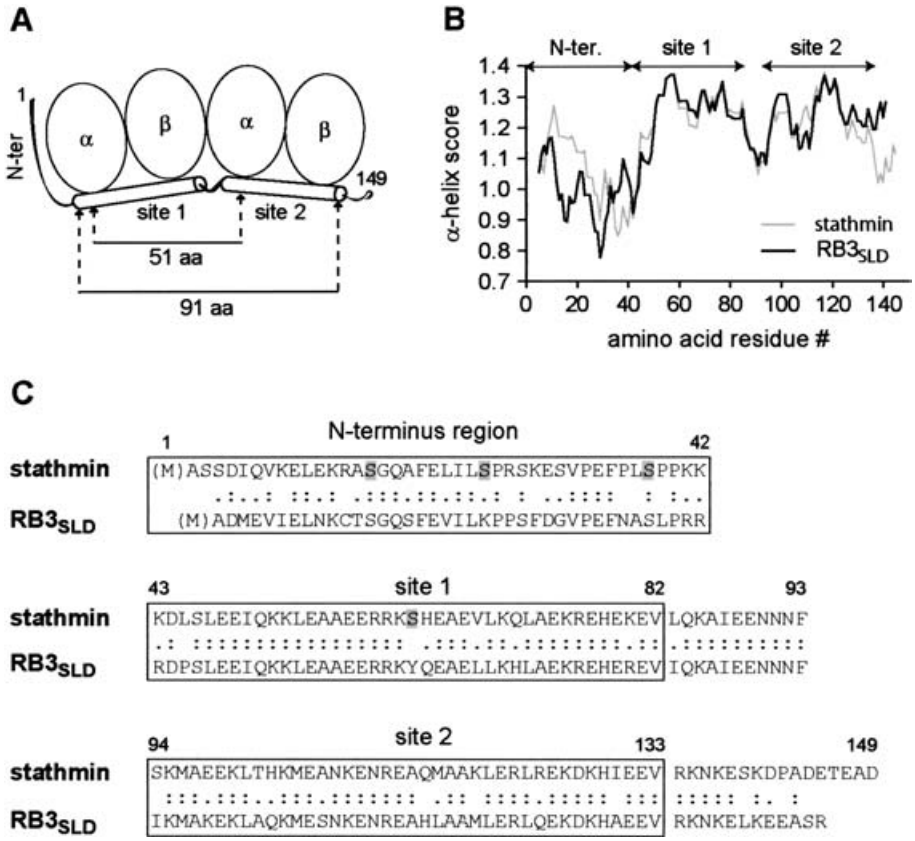

Figure 1 Delimitation of the three main structural regions of the SLDs

(**A**) Model representing the T_2S complex. According to X-ray analysis, the two α/β tubulin heterodimers align head-to-tail along a 91-residue SLD α-helix. The 51 residues spacing corresponds to the distance on the SLD, separating the contact points with the two adjacent α/β tubulin heterodimers. The N-terminal region, which has been shown by cross-linking experiments to interact with α-tubulin, is thought to cap the edging tubulin monomer of the T_2S complex. (**B**) Secondary-structure predictions (algorithm DPM Deleage and Roux) of stathmin (grey) and $RB3_{SLD}$ (black). The SLDs can be divided into three main regions: an N-terminal region and two α-helical regions. The two α-helical regions correspond to the two tubulin-binding sites (sites 1 and 2) (see the Results section). (**C**) The comparison of the stathmin and $RB3_{SLD}$ primary sequences reveals that the most conserved region is site 1 (82.5 % identity, 95 % similarity), followed by site 2 (75 % identity, 90 % similarity) and the N-terminal region (50 % identity, 78.6 % similarity). The two sites are 35 % identical and 69 % homologous in stathmin. Three of the four stathmin phosphorylation sites (grey) are located in the N-terminal region and the last one is in site 1. Those of $RB3_{SLD}$ have not been identified so far. The limits of the three regions were estimated with the stathmin numbering as follows: N-terminus, amino acids 1–42; site 1, amino acids 43–82; site 2, amino acids 94–133.

of SLDs and their functional relationship. To this purpose, we studied the tubulin-binding properties of various fragments and chimaeras of stathmin and $RB3_{SLD}$ using size-exclusion chromatography, SPR (surface plasmon resonance) and tubulin polymerization assays. We demonstrate that the two SLD tubulin-binding sites are not exchangeable and play specific roles in the interaction with tubulin. We further show that the N-terminal region participates in the tubulin sequestration process and that the second C-terminal tubulin-binding site greatly affects the stability of the T_2S complex. Our results indicate that tubulin co-operatively interacts with SLDs and shed a new light towards understanding of the diverse properties of the various SLDs.

MATERIALS AND METHODS

DNA constructs of fragments and chimaeras derived from stathmin and $RB3_{SLD}$

Standard recombinant DNA techniques were performed as described in [31]. All SLD derivatives were expressed using the pET-8c (Novagen, Madison, WI, U.S.A.) and the pDW363 (gift from Dr D. Waugh, Roche Research Center, Nutley, NJ, U.S.A.) inducible expression vectors. Restriction enzymes were from New England Biolabs (Surrey, BC, Canada).

The coding regions of human stathmin [29] and rat $RB3_{SLD}$ [26] cDNAs were used for stathmin and $RB3_{SLD}$ expressions. Truncated SLD derivatives (SN-S1 and RN-R1) were constructed by PCR using the High Expand Fidelity enzyme (Stratagene, La Jolla, CA, U.S.A.). The 5′- and 3′-primers (Genset, Paris, France) contained *Nco*I and *Bam*HI restriction sites respectively to allow the insertion of the amplified product into the expression vectors after *Nco*I and *Bam*HI digestion.

Chimaeras were designed to replace the N-terminal region (N-ter, amino acids 1–42), the first (site 1, amino acids 43–82) or the second (site 2, amino acids 94–133) sites of stathmin by those of $RB3_{SLD}$ or conversely (RN-S1-S2, SN-R1-R2, SN-R1-S2 and SN-S1-R2), or to swap them within stathmin (SN-S1-S1, SN-S2-S2 and SN-S2-S1) (Figure 2). To create junction sites, three restriction sites were introduced with minimum primary sequence change. The *Hpa*I, *Stu*I and *Sna*BI sites were introduced at positions overlapping codons 38, 87 and 134 respectively. Mutational PCRs were performed using the Pfu Turbo DNA polymerase (Stratagene). The subsequently expressed stathmin protein, named stathmin⋆, contained two homologous mutations [S38T ($Ser^{38} \rightarrow$ Thr) and I87L] located at regions

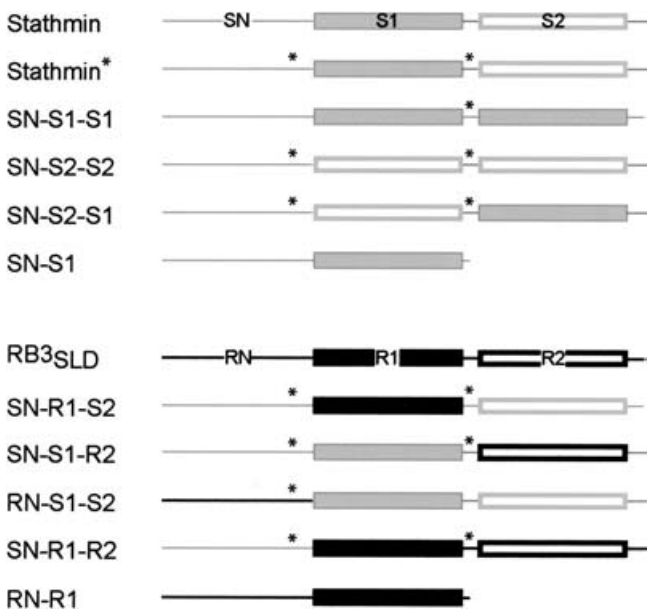

Figure 2 Schematic representation of the various stathmin and $RB3_{SLD}$ derivatives used in this study

Fragments and chimaeras of stathmin (grey = S) or $RB3_{SLD}$ (black = R) were designed to analyse the role played by the N-terminus (N), the first (filled box) and the second (empty box) tubulin-binding sites. The two mutations that were introduced into the stathmin cDNA for the constructions (*) were homologous and coding for residues supposedly not directly involved in the interaction with tubulin (see the Materials and methods section).

supposed to be not involved directly in the interaction with tubulin. stathmin* was checked to display neither shape nor tubulin-binding differences with stathmin, in terms of Stokes radius, *in vitro* tubulin polymerization and complex stability assessed by size-exclusion chromatography (see below). DNAs encoding the first and second sites were made by PCR using 5′- and 3′-primers containing the *Hpa*I, *Stu*I or *Sna*BI restriction sites, depending on the insertion site into the stathmin* DNA.

For SPR experiments, a new coupling approach was developed that allowed a unidirectional, homogeneous and highly stable coupling of SLD derivatives to a streptavidin-coated chip (sensorchip SA; BIAcore AB, Uppsala, Sweden). Recombinant SLD derivatives were expressed using the pDW363-inducible expression vector that directs the synthesis of biotinylated proteins in *Escherichia coli*. pDW363 was designed to fuse a peptide substrate for enzymic biotinylation to the N-terminus of proteins [32]. The substrate was expressed in a coupled translation arrangement with the enzyme. Taking advantage of the presence of the *Xho*I and *Bam*HI sites, the malE region present between these two restriction sites was removed from pDW363 and a linker containing an *Nco*I site was inserted instead. All coding sequences were then subcloned using the *Nco*I and *Bam*HI insertion sites.

All cDNA constructs were checked by sequencing (Genome Express, Meylan, France).

Expression and purification of recombinant stathmin and $RB3_{SLD}$ derivatives

Recombinant proteins were expressed in the BL21(DE3) *E. coli* strain (Stratagene). Luria–Bertani medium (400 ml) containing 100 μg/ml ampicillin was seeded with 1 ml of an overnight preculture and grown at 37 °C. For the growth of bacteria transformed with pDW363, 50 μM biotin was added to the culture. When the exponential phase was reached, the recombinant protein expression was induced by the addition of 0.4 mM isopropyl β-D-thiogalactoside. Bacteria were pelleted 3 h later (at 4000 ***g*** for 15 min at 4 °C) and resuspended in 20 mM Tris/HCl, 1 mM EGTA (pH 8.0), containing the antiprotease cocktail Complete (Roche, Mannheim, Germany). After 1 min sonication for three times on ice, the lysate was centrifuged (4000 ***g*** for 15 min at 4 °C) and the supernatant 1 (S1) was boiled for 10 min and centrifuged again (at 4000 ***g*** for 15 min at 4 °C). This second low-speed supernatant was centrifuged further (100000 ***g*** for 1 h at 4 °C using Optima MAX ultracentrifuge, rotor MLA80; Beckman Instruments, Fullerton, CA, U.S.A.) to yield the boiled S2 supernatant. Boiled S2 supernatants of biotinylated proteins were washed off their biotin by extensive dialysis against PBS, 1 mM EGTA (pH 8.0) and directly used for SPR experiments (see below). The expression of the proteins and the specificity of their biotinylation were verified by SDS/PAGE and Western-blot analysis using streptavidin–horse-radish peroxidase (Molecular Probes, Leiden, The Netherlands).

The S2 supernatants of non-biotinylated proteins were further purified by anion-exchange chromatography. A Q-Sepharose FF column (Amersham Biosciences, Frieburg, Germany) was equilibrated with 20 mM Tris/HCl and 1 mM EGTA (pH 8). Proteins were eluted with a 0–500 mM NaCl linear gradient in the same buffer. The eluted fractions were analysed by SDS/PAGE and Coomassie Blue staining. SLD derivative positive fractions were pooled and concentrated by ultrafiltration using a Centriprep 10 (Millipore, Bedford, MA, U.S.A.). Finally, protein extracts were loaded on to a Superose 12 HR 10/30 size-exclusion chromatography column (Amersham Biosciences) equilibrated with PBS and 1 mM EGTA. The collected fractions and SLD derivative positive fractions were analysed as described above.

Concentrations of the purified protein products were accurately determined by amino acid analysis. For $RB3_{SLD}$, RN-S1-S2 and RN-R1, purification and subsequent experiments were performed in the presence of 1 mM DTT (dithiothreitol) to avoid disulphide bond formation.

Bovine brain tubulin preparation

Tubulin was purified from bovine brain crude extracts by three cycles of polymerization [33], followed by phosphocellulose chromatography [34]. Tubulin was stored at −80 °C in 50 mM Mes/KOH, 0.5 mM DTT, 0.5 mM EGTA, 0.25 mM $MgCl_2$, 0.5 mM EDTA, 3.4 M glycerol and 0.1 M GTP (pH 6.8) for long-term storage. Before use, an additional cycle of polymerization was performed at the end of which tubulin was resuspended in 12.5 mM Mes/KOH, 0.25 mM EGTA and 0.25 mM $MgCl_2$ (pH 6.8). Tubulin concentration was determined by spectrophotometry using a molar absorption coefficient of 115000 M^{-1} cm^{-1} at 280 nm [35].

In vitro tubulin polymerization assay

The effect of different concentrations of SLD derivatives on tubulin polymerization was monitored turbidimetrically at 340 nm [36] in a thermostatically controlled ELISA ThermoMAX spectrophotometer (Molecular Devices, Sunnyvale, CA, U.S.A.). Tubulin alone and tubulin in the presence of stathmin or stathmin* were used as controls. Samples were prepared in buffer M [50 mM Mes/KOH/30 % (v/v) glycerol/6 mM $MgCl_2$/0.5 mM GTP/1 mM EGTA, pH 6.8] and loaded in a half-area transparent 96-well plate (Corning, NY, U.S.A.) with a light path of 0.6 cm. The increase in turbidity was recorded at 37 °C until a plateau was reached. The stationary-state level of polymerization was defined

as the difference between the plateau value and the value at the beginning of the recording. All results are representative of at least two independent experiments.

Gel-filtration assay

The Stokes radii (a) of SLD derivatives were estimated by chromatography at 0.5 ml/min on a Superose 12 HR 10/30 column (Amersham Biosciences) pre-equilibrated with buffer AB (80 mM Pipes/KOH/1 mM EGTA/5 mM $MgCl_2$ pH 6.8) in which 1 mM DTT was added. The total volume (V_t) of the gel bed was determined by loading 1 % acetone and the void volume (V_0) by measuring the elution volume of Blue Dextran. Protein standards used to calibrate the column were from the LMW and HMW gel filtration calibration kits (Amersham Biosciences). Elution volumes (V_e) of samples (20 μg of proteins in 100 μl) were monitored at 226 nm. The Stokes radii of SLD derivatives were estimated on a $(-\log K_{av})^{1/2}$ versus Stokes radius plot, as described by Siegel and Monty [37].

The interaction of the SLD derivatives with tubulin was studied by size-exclusion chromatography on a Superose 12 HR 10/30 column pre-equilibrated with buffer AB at 0.5 ml/min. Monitoring at 278 nm allowed us to observe the tubulin peaks only, since SLD derivatives do not significantly absorb light at this wavelength. Samples of 100 μl containing 10 μM tubulin and various concentrations of SLD derivatives were prepared in buffer AB and loaded on to the column. For SN-S1 and RN-R1, the interaction was favoured by the addition of 1 M TMAO (trimethylamine-*N*-oxide) to the sample and elution buffers and by increasing the tubulin/SLD derivative concentration ratio to 1:6. To search for a shift or a decrease in the SLD derivative elution peak when mixed with tubulin, runs were monitored at 226 nm and 300 μl fractions of either the SLD derivative alone or the SLD derivative plus tubulin were collected to examine their content by Western-blot analysis.

SPR

BIAcore 2000 system, sensorchip SA, and HBS buffer [0.01 M Hepes (pH 7.4)/0.15 M NaCl/3 mM EDTA/0.005 % polyoxyethylenesorbitan] were from BIAcore AB. The sensorchip SA is coated with streptavidin, thus allowing streptavidin–biotin couplings. It was preconditioned with three 10 μl injections of 50 mM NaOH, 1 M NaCl, and saturated with three 10 μl injections of 10 mg/ml BSA. The first flow cell was used as a reference flow cell. The other three flow cells were coupled with the dialysed S2 of the various SLD derivatives that were specifically biotinylated on their N-terminal tag. To obtain surfaces with comparable molecular densities, the amounts of proteins coupled were proportional to their molecular masses. Approx. 140 RU (resonance units) of 18 kDa proteins (e.g. stathmin or chimaeras) and 70 RU of SN-S1 or RN-R1 were coupled. This coupling stage was performed at 10 μl/min in HBS buffer.

To study the interaction of tubulin with the coupled proteins, SPR experiments were performed at a constant flow rate of 30 μl/min, in buffer AB (80 mM Pipes/KOH/1 mM EGTA/5 mM $MgCl_2$ pH 6.8) supplemented with 0.005 % (v/v) P20 surfactant. The interaction with SN-S1 or RN-R1 was favoured by the addition of 1 M TMAO in this buffer. Several runs of tubulin ranging from 1 to 20 μM were made in the presence of 1 mM GDP. The association phase was recorded for 160 s and the dissociation phase for various periods of time. In between two runs, the sensorchip was regenerated with 30 μl of 50 mM Hepes, 500 mM NaCl, 3 mM EDTA and 0.005 % P20 surfactant (pH 7.4).

For the analysis, the reference flow cell sensorgram was subtracted from the corresponding sensorgrams, to abolish base-line drift, bulk and non-specific interaction contributions. These net sensorgrams were then normalized (100 %, maximum signal) to highlight the differences in kinetics.

RESULTS

To understand some of the molecular processes that lead to the formation and stability of tubulin:SLD complexes (generically referred to as T_2S complex), we analysed the role played by three regions of the SLDs in the interaction with tubulin. These regions and their boundaries were estimated according to structural data, sequence comparisons and secondary-structure predictions by dedicated algorithms [38] (Figure 1). The X-ray crystallography of the tubulin:$RB3_{SLD}$ complex revealed that the two tubulin dimers line up along a 91-residue SLD α-helix [21]. A predicted α-helix of corresponding length contains an internal tandem repeat, suggesting that each copy may interact with one tubulin dimer [21,29]. Nevertheless, the two tubulin-interacting sites, while overlapping the repeats, may be larger than the repeats themselves and are designated in the present study as sites 1 and 2. The third region of interest is the N-terminal region of the SLD, which was defined as the region preceding site 1. Therefore we chose to delimit these three regions, using the stathmin numbering, as follows: N-terminal region, amino acids 1–42, site 1, amino acids 43–82 and site 2, amino acids 94–133 (Figure 1).

Characterization of the fragments and chimaeras of stathmin and $RB3_{SLD}$

The contribution of these three regions in the formation and stability of the tubulin:SLD complex was studied by means of fragments and chimaeras of stathmin and $RB3_{SLD}$ in which these specific regions were combined (Figure 2). Fragments and chimaeras were named according to the following nomenclature: N, N-terminus; 1, site 1; 2, site 2. Stathmin-derived sequences were named S, and those from $RB3_{SLD}$, R (e.g. stathmin, SN-S1-S2; $RB3_{SLD}$, RN-R1-R2). Chimaeras were designed to analyse the role of one region in a specific environment. Thus, we constructed stathmin–stathmin chimaeras in which sites 1 and 2 were duplicated (SN-S1-S1 and SN-S2-S2) or inverted (SN-S2-S1), and stathmin-$RB3_{SLD}$ chimaeras where each site of stathmin was replaced by its $RB3_{SLD}$ counterpart (SN-R1-S2, SN-S1-R2, RN-S1-S2 and SN-R1-R2). Fragments were also constructed to compare the effect of truncations in stathmin and in $RB3_{SLD}$ (SN-S1 versus RN-R1).

We ensured by size-exclusion chromatography that all fragments and chimaeras retained the hydrodynamic features of SLDs (Table 1). As described, stathmin and $RB3_{SLD}$ displayed asymmetrical and elongated shapes because their apparent molecular masses are larger than their calculated molecular masses [28]. The fragments derived from $RB3_{SLD}$ had lower Stokes radii and lower apparent molecular masses when compared with the stathmin fragments. Thus they retained the relative hydrodynamic characteristics of $RB3_{SLD}$ and stathmin respectively. The Stokes radii and apparent molecular masses of the chimaeras were all in the same order of magnitude as those of stathmin [approx. 38 Å (1 Å = 0.1 nm) and 70 kDa]. Hence, their global organization was not altered. Importantly, differences in size-exclusion chromatography elution profiles of the complexes with tubulin could not be accounted for by different Stokes radii of their SLD components, but rather reveal differences in tubulin binding.

Table 1 Stokes radii and apparent molecular masses of the recombinant SLD derivatives

A Superose 12 gel-filtration column was calibrated with a series of standard proteins. Stokes radii (a) and apparent molecular masses (M_{app}) of the recombinant SLD derivatives were deduced from their elution volumes (see the Materials and methods section). M_{cal} is the calculated molecular mass determined from amino acid sequences. M_{app}/M_{cal} ratio is presented as an indication of the protein asymmetry.

Protein	a(Å)	M_{app}	M_{cal} (kDa)	M_{app}/M_{cal}
Stathmin	38.7	75.4	17.3	4.3
Stathmin⋆	38.7	75.4	17.3	4.3
$RB3_{SLD}$	32.0	45.4	17.0	2.6
SN-S1-S1	37.7	70.1	17.3	4.0
SN-S2-S2	38.1	71.8	17.3	4.1
SN-S2-S1	36.8	65.5	17.3	3.8
SN-R1-S2	38.5	74.1	17.4	4.2
SN-S1-R2	37.8	70.5	17.2	4.1
S1-S2	30.8	41.2	11.4	3.6
R1-R2	26.3	28.7	11.2	2.6
SN-S1	29.9	38.5	10.1	3.8
RN-R1	28.3	33.8	10.2	3.3

TMAO is an efficient stabilizer of the T_2S complexes

TMAO is a natural osmolyte that stimulates tubulin polymerization and lowers the tubulin critical concentration by structuring and stabilizing tubulin [39]. Therefore we wondered whether it could favour the interaction between tubulin and SLDs and be a helpful tool for studying low-stability complexes. Its effect on the tubulin:stathmin interaction was studied by size-exclusion chromatography (Figure 3). In the absence of TMAO, the tubulin peak shifted by stathmin displayed a trailing shoulder corresponding to tubulin partially dissociated from stathmin [19,28]. In contrast, in the presence of TMAO, a single tubulin peak was observed, showing that the complex was stabilized. The stabilizing effect of TMAO was even more obvious with $RB3'_{SLD}$, an RB3 splice variant that forms a T_2S complex of poor stability with tubulin [28]. Indeed, in the absence of TMAO, the tubulin:$RB3'_{SLD}$ complex was not stable, the tubulin peak being only slightly shifted when compared with that induced by stathmin. The addition of 1 M TMAO led to a marked shift of the tubulin resembling that of the tubulin:stathmin complex. Thus TMAO appears as a good tool for the comparative study of low-stability complexes.

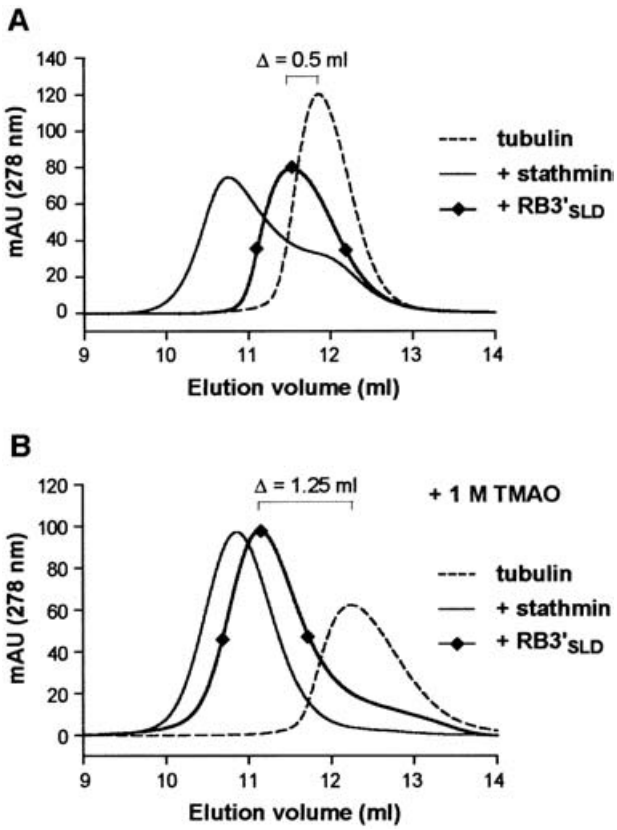

Figure 3 TMAO favours the tubulin:SLD interactions

Size-exclusion chromatography assays were performed in the absence (**A**) or in the presence (**B**) of 1 M TMAO and were monitored at 278 nm. Tubulin (10 μM) was loaded on to a Superose 12 column, either alone (broken line) or in the presence of 5 μM stathmin (solid line) or $RB3'_{SLD}$ (◆). The shift of the tubulin peak induced by $RB3'_{SLD}$ is indicated (Δ).

Each stathmin site plays a specific role in the interaction of stathmin with tubulin

The two sites of stathmin each contain a copy of an internal tandem repeat. This sequence similarity may be relevant to the binding of the two identical tubulin heterodimers. To explore the extent to which these two sites play similar or distinct roles in the interaction with tubulin, we analysed the tubulin-binding properties of stathmin–stathmin chimaeras in which the first and the second sites were duplicated (SN-S1-S1 and SN-S2-S2) or swapped (SN-S2-S1) (Figure 2).

Stathmin–stathmin chimaeras retain the ability to bind two tubulin heterodimers

The functionality of these chimaeras to form T_2S complexes was tested by size-exclusion chromatography under optimized conditions, i.e. in the presence of 1 M TMAO. Tubulin (10 μM) was loaded either alone or as a mixture with stathmin⋆ or 5 μM chimaeras. As illustrated in Figure 4(A), SN-S1-S1 and SN-S2-S2 formed complexes that were mostly eluted at the same volume as the tubulin:stathmin⋆ complex.

Under the same conditions, SN-S2-S1 induced a shift of the tubulin peak but far less than stathmin⋆ (Figure 4B), a peak of nearly equal surface remaining eluted at the free tubulin elution volume, implying that only half the available tubulin was bound by SN-S2-S1. This could signify either that SN-S2-S1 retained only one functional site (real TS complex) or that the two sites were transiently occupied. The latter was privileged because runs performed with higher concentrations of this chimaera (20 and 40 μM) induced a better shift of the tubulin peak, and because both SN-S1-S1 and SN-S2-S2 could effectively bind two tubulin heterodimers.

Thus, inasmuch as they can form T_2S complexes under optimized conditions, we conclude that SN-S1-S1, SN-S2-S2 and SN-S2-S1 retain some of the essential tubulin sequestration properties of stathmin.

The two tubulin-binding sites of stathmin are not interchangeable and their efficiency of tubulin sequestration depends on their location in the SLD

We compared the affinity of each one of SN-S1-S1, SN-S2-S2 or SN-S2-S1 for tubulin, with *in vitro* tubulin-polymerization assays (Figure 5A). In the presence of 1 mol of a T_2S-forming protein, the tubulin-polymerizable pool would be depleted by 2 mol of tubulin.

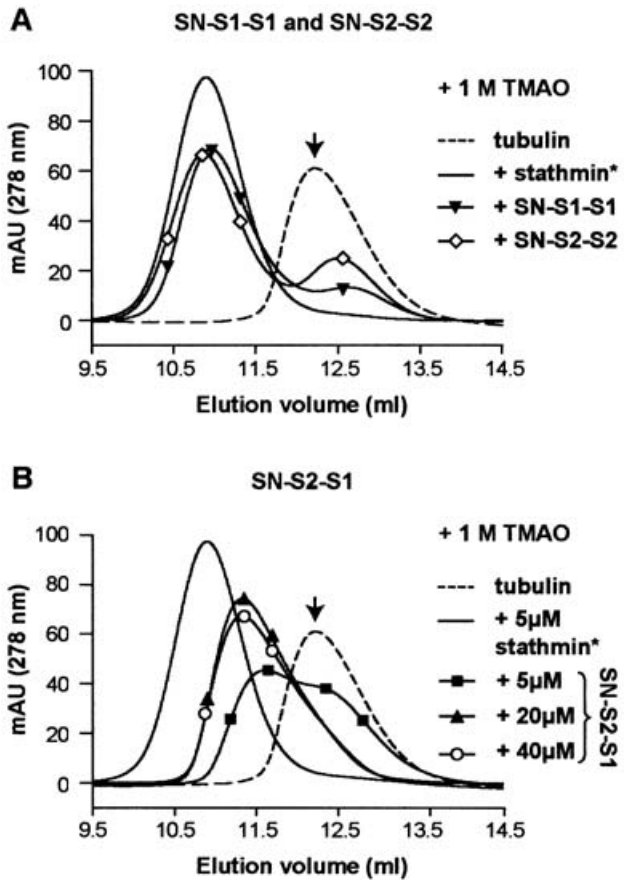

Figure 4 The ability of SN-S1-S1, SN-S2-S2 and SN-S2-S1 to form T_2S complexes revealed by size-exclusion chromatography in the presence of TMAO

(**A**) Elution profiles of 10 μM tubulin alone (broken line) or mixed with 5 μM stathmin* (solid line), SN-S1-S1 (▼) or SN-S2-S2 (◇). These two chimaeras probably bind two tubulin heterodimers, since they form complexes with tubulin that are eluted similarly to the tubulin:stathmin* complex. (**B**) Elution profiles of various concentrations of SN-S2-S1 mixed with 10 μM tubulin. The tubulin peak is more shifted in the presence of higher concentrations of SN-S2-S2. The ability of SN-S2-S1 to bind two tubulin heterodimers is further supported by the fact that SN-S1-S1 and SN-S2-S2 are functional regarding tubulin sequestration. Experiments were performed in buffer AB (see the Materials and methods section) + 1 M TMAO. Arrows show the excess of free tubulin as revealed by monitoring at 278 nm, probably due to the low stability of the complexes.

Thus we calculated and plotted the microtubule plateau values that should be obtained with 20 μM tubulin and various concentrations of such a T_2S-forming protein. This theoretical T_2S plot indicates the saturation level of the tubulin-binding sites ($T_2S = 100\%$). Then, 20 μM tubulin was allowed to polymerize in the presence of various concentrations of stathmin* or of the three stathmin–stathmin chimaeras. The stathmin* and the SN-S1-S1 tubulin polymerization plots fitted with the theoretical T_2S plot, implying that their two tubulin-binding sites were 100% saturated with tubulin. In contrast, SN-S2-S2 and SN-S2-S1 inhibited tubulin polymerization with lower efficiency (80 and 50% respectively). As we showed that each chimaera was able to bind two α/β tubulin heterodimers, the differences observed in the present study reflect the affinities of the chimaeras for tubulin [40]. These chimaeras could thus be qualitatively classified according to their affinities as follows: stathmin* ≈SN-S1-S1 > SN-S2-S2 > SN-S2-S1.

Differences between the various tubulin:chimaera complexes were further examined by SPR. Figure 5(B) shows the normalized signals obtained with 5 μM tubulin. The apparent associations of

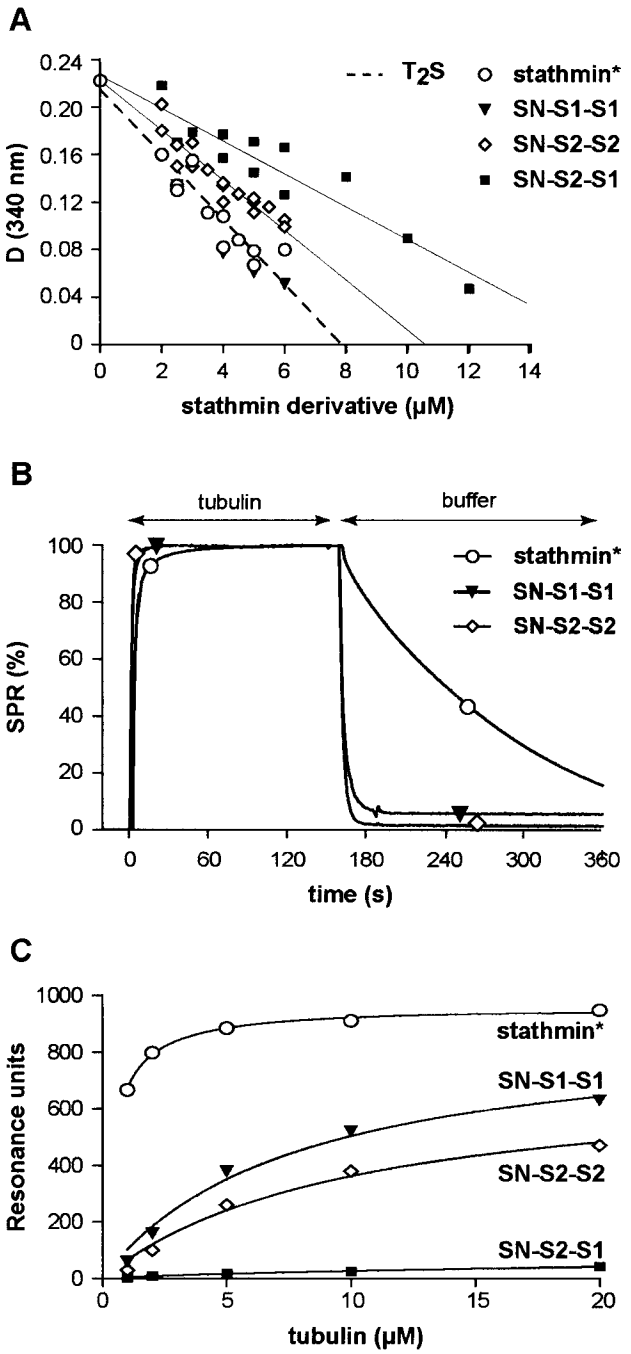

Figure 5 Evidence for the different but complementary roles of the two stathmin sites

(**A**) Tubulin polymerization was performed at 37 °C for 1 h and microtubule assembly was monitored by turbidimetry at 340 nm (*D*, attenuance). The T_2S plot is a theoretical plot that represents the maximum saturation level of the two tubulin-binding sites (see text). Tubulin (20 μM) was allowed to polymerize in the presence of different concentrations of stathmin* as a control (○), SN-S1-S1 (▼), SN-S2-S2 (◇) or SN-S2-S1 (■). The results show that the chimaeras inhibit tubulin polymerization with approx. 100, 80 and 50% efficiencies respectively. (**B**) SPR was assessed by coupling stathmin* or chimaeras on streptavidin-coated sensorchips (SA) via an N-terminal biotinylated tag and injecting various concentrations of tubulin. Tubulin was injected for 160 s (tubulin, association phase), and the dissociation phase (buffer) was monitored for 200 s. The net normalized signals for an injection of 5 μM tubulin are presented. Tubulin associates with and dissociates from SN-S1-S1 (▼) and SN-S2-S2 (◇) much faster than from stathmin* (○). (**C**) Saturation curves were drawn from the maximum RU measured during the association phase as a function of tubulin concentration. Chimaeras can be qualitatively classified according to their affinity for tubulin, as follows: stathmin* > SN-S1-S1 > SN-S2-S2 > SN-S2-S1.

Table 2 Tubulin half dissociation time constants for the various SLD derivatives

The half dissociation times ($t_{1/2}$) were graphically deduced from SPR signals obtained with 5 μM tubulin. The $t_{1/2}$:$t_{1/2}$ stathmin* ratio is indicated to compare the dissociation behaviour of tubulin with the SLD derivatives and with stathmin*. Abbreviation: n.d., not determined.

Protein	$t_{1/2}$ (s)	$t_{1/2}/t_{1/2}$ stathmin*
Stathmin*	63	1
SN-S1-S1	< 2	< 0.03
SN-S2-S2	< 2	< 0.03
SN-S2-S1	n.d.	n.d.
SN-R1-S2	69	1.1
RN-S1-S2	74	1.2
$RB3_{SLD}$	1070	17.9
SN-S1-R2	540	8.6
SN-R1-R2	1790	28.4

tubulin with SN-S1-S1 and SN-S2-S2 appeared slightly faster than that with stathmin*, and tubulin dissociated almost instantly from the two chimaeras, i.e. much faster than from stathmin* (Table 2). Hence, as the apparent association kinetics is the net result from both the actual association and dissociation rates, the actual association rates of the chimaeras must be much faster than that of stathmin* to balance the concomitant fast dissociation rates. However, these normalized plots did not allow us to discriminate SN-S1-S1 from SN-S2-S2 regarding tubulin kinetics. This was done by plotting the maximum RU measured during the association phase as a function of tubulin concentration (Figure 5C). The resulting saturation curves clearly show that SN-S1-S1 had a higher affinity for tubulin when compared with SN-S2-S2, but much lower than stathmin*, and that SN-S2-S1 had the lowest affinity. Thus the present study extends the size-exclusion chromatography and tubulin polymerization results and lead to a finer relative affinity ordering: stathmin* $\gg$ SN-S1-S1 > SN-S2-S2 $\gg$ SN-S2-S1.

In conclusion, our results show that replacing site 1 by site 2 and vice versa in stathmin decreases the efficiency of tubulin binding.

Regions responsible for the different tubulin-binding properties of stathmin and $RB3_{SLD}$

Like stathmin, $RB3_{SLD}$ is capable of binding two tubulin heterodimers, but displays very different tubulin-binding kinetics [28], $RB3_{SLD}$ forming a more stable complex with tubulin. We took advantage of these differences to determine the role of the three regions of the SLDs in the mechanistic events that take place in the SLD for the formation and stability of the T_2S complex.

Site 2 is a major stabilizing component of the T_2S complex

We analysed the influence of each site on the differences between stathmin and $RB3_{SLD}$ by replacing either site 1 or site 2 of stathmin by that of $RB3_{SLD}$ (SN-R1-S2 and SN-S1-R2).

Tubulin polymerization assays showed that the two chimaeras retained their functionality, since they behave like T_2S-forming proteins (Figure 6A).

We then compared the stabilities of these complexes by size-exclusion chromatography. Figure 6(B) presents the elution profiles of 10 μM tubulin alone or with 5 μM stathmin*, $RB3_{SLD}$ or chimaeras. Both chimaeras induced a shift of the tubulin peak. Whereas the tubulin:SN-R1-S2 complex was eluted at the same position as the tubulin:stathmin complex, SN-S1-R2 induced a better shift of the tubulin peak.

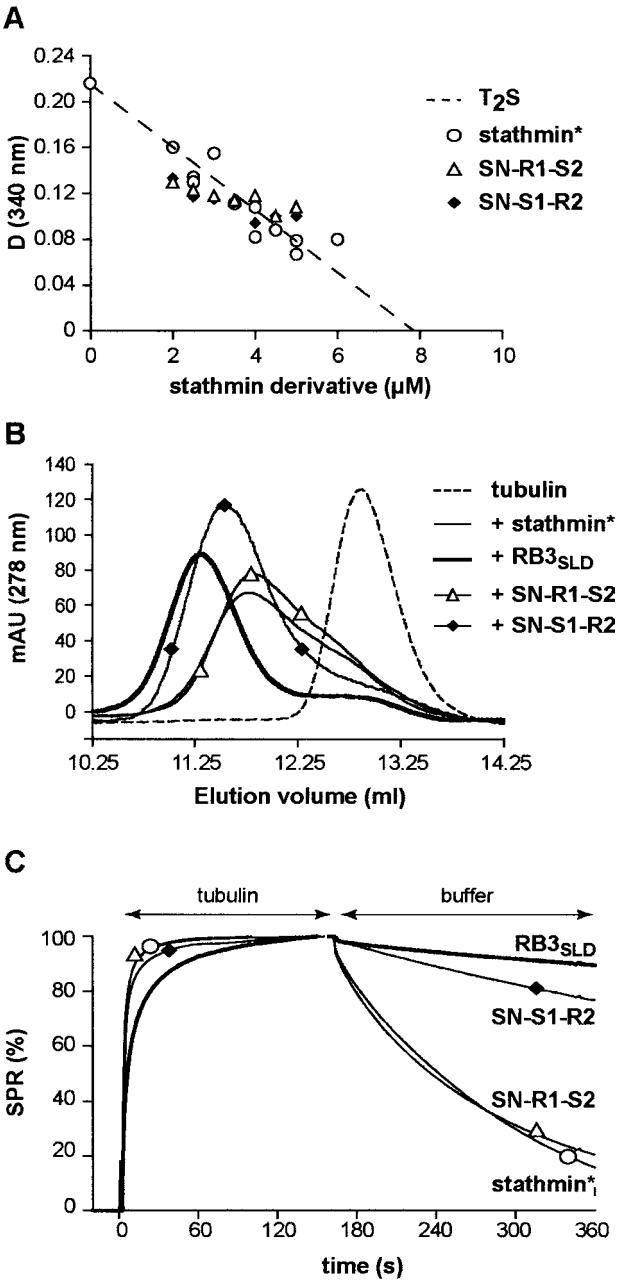

Figure 6 SN-S1-R2, but not SN-R1-S2, diverges from the stathmin* behaviour regarding tubulin sequestration

(**A**) Inhibition of tubulin polymerization by the SN-S1-R2 and SN-R1-S2 chimaeras *in vitro*. The amounts of microtubules at steady state obtained with 20 μM tubulin in the presence of various concentrations of stathmin derivatives are reported. The SN-S1-R2 (◆) and SN-R1-S2 (△) plots fit with the theoretical T_2S plot. (**B**) Gel-filtration profiles of tubulin monitored at 278 nm from samples containing 10 μM tubulin, either alone (broken line) or with 5 μM SN-R1-S2 (△), SN-S1-R2 (◆), stathmin* (thin black) or $RB3_{SLD}$ (thick black). Globally, as a matter of shape and elution volume, the SN-R1-S2 peak resembles that of stathmin* and the SN-S1-R2 peak that of $RB3_{SLD}$. (**C**) SPR signals observed when injecting 5 μM tubulin on immobilized stathmin* (○), $RB3_{SLD}$ (thick black), SN-R1-S2 (△) and SN-S1-R2 (◆). The SN-R1-S2 curve is similar to the stathmin* curve, whereas the SN-S1-R2 curve diverges from it and tends to resemble that of $RB3_{SLD}$.

These results were extended by SPR analysis (Figure 6C). The apparent association and dissociation kinetics of tubulin with

SN-R1-S2 and stathmin* appeared similar. On the other hand, the half dissociation time of tubulin from SN-S1-R2 (540 s) was much longer than from stathmin* (63 s) (Table 2). The association of tubulin with SN-S1-R2 also appeared slower than that of tubulin with stathmin*, especially when corrected for the concomitant dissociations.

Thus replacing site 1 of stathmin by site 1 of $RB3_{SLD}$ induced almost no change in the association and dissociation kinetics of tubulin. More remarkably, introducing the second $RB3_{SLD}$ site into stathmin shifted the tubulin interaction kinetics and stability of stathmin towards those of $RB3_{SLD}$.

The N-terminal regions of stathmin and $RB3_{SLD}$ participate in the tubulin sequestering process but with different efficiencies

The influence of the N-terminal region was assessed by the comparison of RN-S1-S2 with stathmin and that of SN-R1-R2 with $RB3_{SLD}$. At first glance, the kinetics of tubulin binding to RN-S1-S2 and SN-R1-R2 resembled those of tubulin binding to stathmin* and $RB3_{SLD}$ respectively (Figure 7A). In particular, the apparent association with RN-S1-S2 and stathmin appeared very similar and the determination of the half dissociation times did not reveal further differences (Table 2). However, the apparent association with SN-R1-R2 appeared slightly faster when compared with $RB3_{SLD}$, and the half dissociation time (1790 s) was larger when compared with that from $RB3_{SLD}$ (1070 s). This indicates that the N-terminal region is probably involved in the sequestering process and that the N-terminal regions of stathmin and $RB3_{SLD}$ behave differently.

Because the stabilizing effect of the second tubulin-binding sites (see Figure 6) might have hidden the influence of the N-terminal regions, we removed these sites by comparing SN-S1 and RN-R1. We first analysed SN-S1 and RN-R1 by SPR experiments in the presence of 1 M TMAO. Figure 7(B) represents the net sensorgrams obtained with a range of tubulin concentrations. SN-S1 clearly bound much more tubulin when compared with RN-R1. Tubulin interaction kinetics with SN-S1 were very rapid, since tubulin associated and dissociated extremely fast, whereas tubulin associated to and dissociated from RN-R1 very slowly.

These results were extended by comparing the affinities of SN-S1 and RN-R1 for tubulin with *in vitro* tubulin polymerization assays (Figure 8A). In this case, the maximum efficiency (100%) of tubulin polymerization inhibition was obtained when the single tubulin-binding site was fully saturated with one tubulin heterodimer. The two SLD derivatives were capable of limiting tubulin polymerization but SN-S1 did so more efficiently when compared with RN-R1 (approx. 85 and 70% saturation respectively), indicating that SN-S1 has a higher affinity for tubulin when compared with RN-R1.

Finally, the interaction of SN-S1 or RN-R1 with tubulin was tested by size-exclusion chromatography in the presence of 1 M TMAO. As these SLD derivatives are small and expected to bind a single tubulin heterodimer, the complexes made with tubulin were probably eluted like uncomplexed tubulin. For this reason, we focused on the observation of the SLD derivative peaks by monitoring at 226 nm. Fractions from the column corresponding to the tubulin and SLD derivative peaks were collected and analysed by Western-blot analysis. Figure 8(B) shows that in the presence of tubulin, the SN-S1 peak was barely shifted and its surface was not diminished, reflecting the rapid equilibrium observed by SPR. In contrast, RN-R1 was partly eluted in the same fractions as tubulin and the RN-R1 peak was shifted as well as reduced (Figure 8C). The tubulin:RN-R1 complex appeared more stable when compared with the one formed with SN-S1, again confirming the SPR observations.

In conclusion, SN-S1 seems to have a higher affinity for tubulin when compared with RN-R1, but the complex is far less stable than the one obtained with RN-R1.

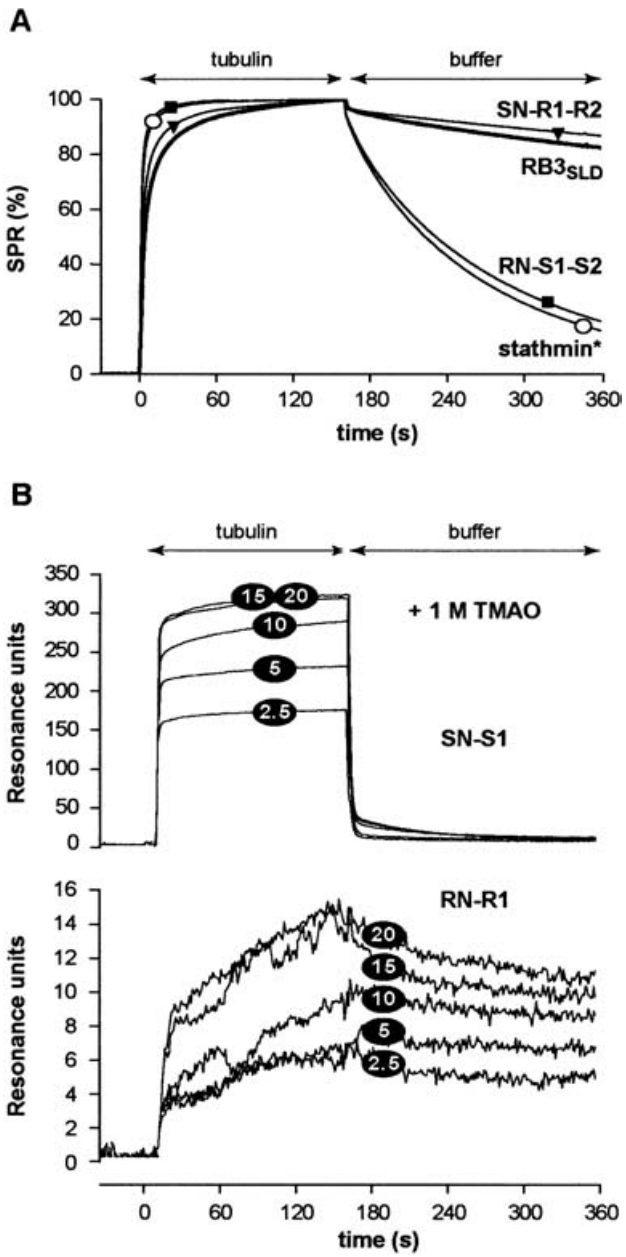

Figure 7 Different influences of the N-terminal regions of stathmin and $RB3_{SLD}$ on tubulin binding

(**A**) SPR-normalized signals obtained for 5 μM tubulin binding to immobilized stathmin* (○), $RB3_{SLD}$ (thick black), RN-S1-S2 (■) and SN-R1-R2 (▼). The presence of the N-terminal region of stathmin in the $RB3_{SLD}$ sequence allows the formation of the most stable complex observed in this study, whereas RN-S1-S2 behaves like stathmin* regarding tubulin association and dissociation. (**B**) SPR 'net' sensorgrams (BSA reference subtracted) obtained for tubulin binding to immobilized SN-S1 (upper panel) or RN-R1 (lower panel). The interaction was favoured by the presence of 1 M TMAO. Approx. 70 RU of fragments and 140 RU of control $RB3_{SLD}$ (results not shown) were immobilized on the sensorchip (see Figure 5B). Tubulin was injected for 160 s and the dissociation phase was monitored for 240 s. The concentrations of tubulin are indicated. Note the difference in scale between the upper and lower panels. SN-S1 binds significant amounts of tubulin with rapid kinetics, whereas RN-R1 binds very few tubulins with slow kinetics.

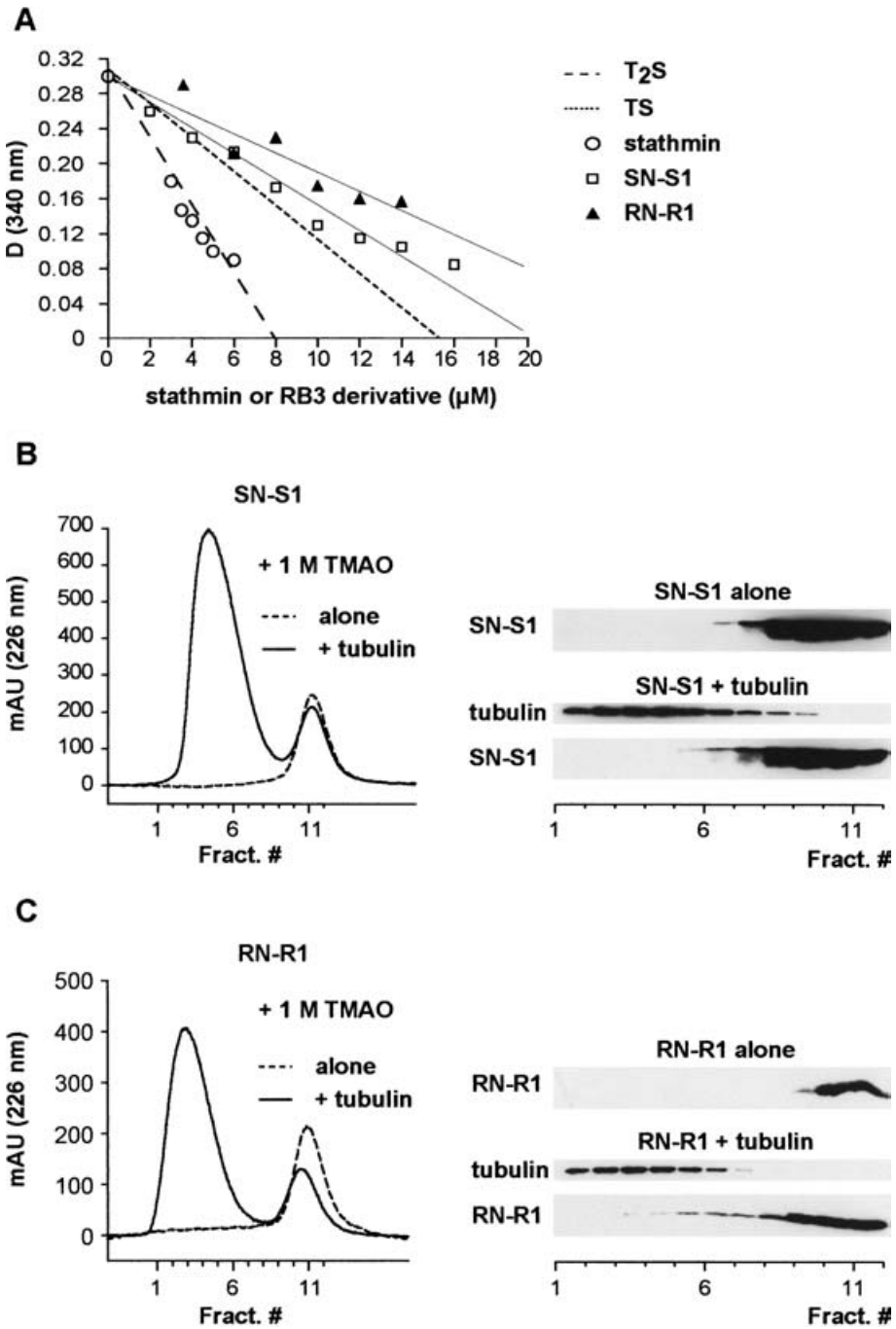

Figure 8 SN-S1 and RN-R1 display different tubulin-binding properties

(**A**) Effect of SN-S1 and RN-R1 on tubulin polymerization *in vitro*. The experimental conditions were the same as those described in Figure 5(A). The theoretical plot corresponding to the full sequestration of one tubulin heterodimer by a single tubulin-binding site is shown (dotted line). Thus 100 % represents the maximum saturation of a single tubulin-binding site (TS = 100 %). SN-S1 (□) and RN-R1 (▲) are approx. 85 and 70 % saturated with tubulin respectively. For comparison, the plot that would be obtained in the presence of a protein containing two tubulin sites that would fully sequester tubulin (T_2S) is reported (dashed line) and stathmin (○) was used as a control. (**B**, **C**). Size-exclusion chromatography profiles of SN-S1 (**B**) and RN-R1 (**C**) alone (broken line) or in the presence of tubulin (continuous line). To favour the interaction, runs were achieved in the presence of 1 M TMAO. SLD derivative (60 μM) was incubated with 10 μM tubulin before being applied to a Superose 12 column (left panel). Western-blot analysis of the collected fractions (right panel) showed that the RN-R1 peak is shifted in the presence of tubulin, and that SN-S1 remains eluted at its control volume.

DISCUSSION

Stathmin is a ubiquitous cytosolic phosphoprotein that regulates microtubule dynamics by sequestering tubulin in a complex consisting of two α/β tubulin heterodimers per stathmin molecule (T_2S). The process of tubulin sequestration most probably accounts for the effect of stathmin on microtubule dynamics. The other proteins of the stathmin family can also sequester tubulin through their SLD, but the different T_2S complexes display very different stabilities. To describe better the mechanistic processes that lead to the sequestration of tubulin and to progress in the understanding of this diversity, we analysed the relative influence

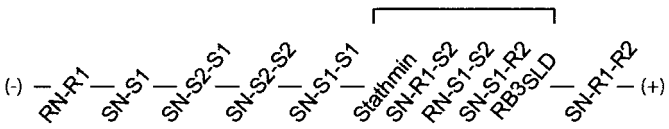

Figure 9 Relative affinity scale of tubulin:SLD derivatives

The relative affinities of the various tubulin:SLD derivative complexes used in this study were determined based on the converging results obtained by *in vitro* tubulin polymerization, SPR and size-exclusion chromatography assays (see text). (−), Low affinity; (+) high affinity. When these techniques did not allow us to differentiate constructs regarding their affinities for tubulin (bracket), they were classified according to the relative stability of the complexes that they formed with tubulin. The best affinity for tubulin is observed in the group of constructs in which both sites 1 and 2 are present and located at positions 1 and 2 respectively. Specific combinations between the N-terminal region, sites 1 and 2 of stathmin and $RB3_{SLD}$ induce changes in the affinity for tubulin, the optimum affinity being observed with SN-R1-R2.

of three regions of SLDs on the interaction with tubulin. To do so, we used *in vitro* tubulin polymerization assays that directly revealed affinity differences as shown by Amayed et al. [40], SPR data that provided half dissociation times reflecting k_d and indirect evaluations of k_a from the apparent association patterns, and size-exclusion chromatography assays that gave information about complex stability. The various SLD derivatives used in this study were thus ordered according to their relative affinities for tubulin, as presented in Figure 9.

Relative roles of the N-terminus, the first and the second sites of stathmin in its interaction with tubulin

The two tubulin-binding sites of stathmin each contain a copy of an internal tandem repeat. Despite these apparent similarities, we found, using stathmin–stathmin chimaeras, that these two sites are not equivalent since replacing site 1 by site 2 and vice versa (SN-S1-S1 and SN-S2-S2) altered the tubulin-binding characteristics of stathmin. In addition, the contribution of each site appears to depend on its location within the molecule. This is best exemplified by SN-S2-S1, which contains the three regions of stathmin but displays the lowest affinity for tubulin and formed the least stable complex. Hence, sites 1 and 2 must play distinct but complementary roles in the formation and stability of the T_2S complex and their relationship with the other regions must be of importance.

This raises the question of the relationship between the N-terminal region and site 1, since these two regions interact with the same tubulin heterodimer in the T_2S complex [21,30]. Our results show that when site 1 is preceded by the N-terminal region, it is capable of forming a complex of very low affinity with tubulin. This could explain why previous attempts to detect an interaction between site 1 alone and tubulin have failed [20,23,41]. Interestingly, SN-S1-S1 has a higher relative affinity for tubulin when compared with SN-S2-S2. At first sight this suggests that site 1 binds tubulin with a better affinity when compared with site 2, but SN-S2-S1 did not display a better affinity when compared with SN-S2-S2. Instead, one could rather consider that SN-S1-S1 is the only chimaera of this series where the N-terminal region remained associated with site 1. This indicates that one tubulin heterodimer may need to be correctly bound to the N-terminal region+site 1 to favour the binding of the other tubulin heterodimer. Thus the binding of tubulin to the N-terminal region+site 1 may constitute the primary and determinant event of the T_2S complex formation.

Regarding site 2, we showed that its replacement by site 1 greatly decreases the stability of the complex formed with tubulin. The second site appears as a stabilizing component of the tubulin:stathmin complex.

Our findings provide direct evidence for a positive co-operativity model [40]. Indeed, we show that the N-terminal region is necessary for site 1 to bind a first tubulin heterodimer. Although this interaction is very weak, it influences the binding of the second tubulin on site 2, which in turn participates in the stabilization of the whole T_2S complex.

Molecular basis for the differences in tubulin-binding properties of SLDs

Beyond the description of the tubulin:stathmin interaction, our results further allow us to identify regions responsible for the different tubulin-binding properties displayed by stathmin and $RB3_{SLD}$.

The very similar behaviours of SN-R1-S2 and stathmin indicated that the first sites of $RB3_{SLD}$ and stathmin perform similar roles in the formation of the T_2S complex. Hence, the comparison of SN-S1 and RN-R1 should reveal differences between the N-terminal regions. Indeed, SPR experiments showed that the tubulin:SN-S1 complex is in rapid equilibrium in contrast with the tubulin:RN-S1 complex, and tubulin polymerization assays showed that SN-S1 has a higher affinity for tubulin. This suggests that the N-terminal region does not favour the binding of tubulin in $RB3_{SLD}$ as well as in stathmin. Finally, the comparison of SN-S1-R2 with stathmin showed that the second site of $RB3_{SLD}$ is also a T_2S-complex stabilizer, even more efficient than that of stathmin. This is in agreement with the observation that $RB3'_{SLD}$, a C-terminal truncated variant of $RB3_{SLD}$, forms a very low-stability complex with tubulin [28].

This indicates that the N-terminal region and the second site, but not the first site, are responsible for the bulk tubulin-binding differences between stathmin and $RB3_{SLD}$. Interestingly, this is in accordance with the primary sequence conservation of these regions between stathmin and $RB3_{SLD}$ (Figure 1) that lie in the order: site 1 (82.5% identity) > site 2 (75% identity) > N-terminal region (50% identity). Moreover, a relative balance seems to exist between the N-terminal region and the second site, which would be opposite in stathmin and in $RB3_{SLD}$. Indeed, the N-terminal region of stathmin favours the interaction with tubulin better than that of $RB3_{SLD}$, whereas the second site of $RB3_{SLD}$ stabilizes the interaction better than stathmin. This hypothesis is also supported by the fact that SN-R1-R2 displays a better affinity for tubulin when compared with $RB3_{SLD}$. Curiously, RN-S1-S2 practically behaved like stathmin and did not slow down tubulin association. The N-terminal region of $RB3_{SLD}$ might have so little influence on tubulin binding that it is compensated by site 2 in RN-S1-S2 as it is in $RB3_{SLD}$. But it is also possible that the combination of a given N-terminal region and a given site 1 induces a specific association rate. In such a hypothesis, RN combined with R1, but not RN alone, could be the reason why $RB3_{SLD}$ associates slowly with tubulin.

Biological significance

The fact that the N-terminal region and site 2 do not play the same relative roles in stathmin and in $RB3_{SLD}$ for the interaction with tubulin suggests that this interaction is differentially regulated. The four stathmin phosphorylation sites are located in the N-terminal region + site 1 and their combinatory phosphorylation can greatly alter the stability of the complex formed with tubulin [5,6,18]. The phosphorylation of stathmin could alter the binding of the first tubulin, possibly by provoking local unfolding [42], which could make the subsequent co-operative events difficult to occur. Although little is known about the phosphorylation of

$RB3_{SLD}$, the fact that three of the four phosphorylation sites of stathmin are poorly conserved in $RB3_{SLD}$ suggests that the interaction with tubulin is not regulated by the phosphorylation of the N-terminus + site 1 region to any great extent. Nevertheless, the other serine residues are spread all over the $RB3_{SLD}$ sequence. Notably, residue 107 located in site 2 could be phosphorylated by CKII or by PKC to control the stability of the T_2S complex, which is strongly dependent on site 2. Therefore RB3 may be phosphorylated by different kinases when compared with those phosphorylating stathmin in response to different signals and leading to different cellular responses, such as a kinetically longer or stronger sequestration of tubulin.

It is noteworthy that apart from stathmin, all proteins of the stathmin family display various extensions positioned N-terminal to the SLD. These extensions are responsible in particular for their attachment to membranes [43]. They might alter the interaction with tubulin or its regulation, e.g. by steric hindrance or structural arrangements. One adaptation could have been to make the stability of the tubulin:SLD complexes mostly dependent on site 2. This adaptation could have been an opportunity for the phosphoproteins of the stathmin family to be regulated depending on their location in the cell and to play possible different or complementary roles in various intracellular compartments. *In vivo* studies aimed at analysing the activity of the proteins of the stathmin family in relation to their location should be instrumental in testing these hypotheses.

In conclusion, our results highlight the molecular processes by which tubulin co-operatively interacts with the SLDs. We show that the N-terminal region of stathmin takes part in the sequestering process for the binding of the first tubulin heterodimer to site 1. This seems to facilitate the binding of a second tubulin heterodimer on site 2, an event that in turn may stabilize the whole T_2S complex. We also showed that the N-terminal region and site 2 do not have the same relative influence on stathmin and RB3 for the binding of tubulin, a property that might permit differential regulation by phosphorylation. Finally, considering that stathmin is highly overexpressed in numerous cancers [14–17], our results of the present study might contribute to the design of high-affinity peptides that could mimic or compete with SLDs, thus modifying the SLD–tubulin equilibrium, which is expected to slow down the cell cycle and to be useful for the treatment of cancer.

We thank P. Amayed (LEBS) for her help in preparing bovine brain tubulin. We are grateful to J. M. Camadro (Institut Jacques Monod, Paris, France) for technical help with the BIAcore experiments and to D. Waugh for the gift of the pDW363 expression vector. We thank O. Gavet, S. Chauvin and R. Rudge for a critical reading of the manuscript. This work was supported by Institut National de la Santé et de la Recherche Médicale, Association pour la Recherche sur le Cancer, Association Française contre les Myopathies and Ligue Nationale contre le Cancer.

REFERENCES

1 Sobel, A., Boutterin, M. C., Beretta, L., Chneiweiss, H., Doye, V. and Peyro-Saint-Paul, H. (1989) Intracellular substrates for extracellular signaling: characterization of a ubiquitous, neuron-enriched phosphoprotein (Stathmin). J. Biol. Chem. **264**, 3765–3772

2 Hailat, N., Strahler, J. R., Melhem, R. F., Zhu, X. X., Brodeur, G., Seeger, R. C., Reynolds, C. P. and Hanash, S. M. (1990) N-myc gene amplification in neuroblastoma is associated with altered phosphorylation of a proliferation related polypeptide (Op 18). Oncogene **5**, 1615–1618

3 Belmont, L. D. and Mitchison, T. J. (1996) Identification of a protein that interacts with tubulin dimers and increases the catastrophe rate of microtubules. Cell (Cambridge, Mass.) **84**, 623–631

4 Marklund, U., Larsson, N., Melander Gradin, H., Brattsand, G. and Gullberg, M. (1996) Oncoprotein 18 is a phosphorylation-responsive regulator of microtubule dynamics. EMBO J. **15**, 5290–5298

5 Horwitz, S. B., Shen, H.-J., He, L., Dittmar, P., Neef, R., Chen, J. and Schubart, U. K. (1997) The microtubule-destabilizing activity of metablastin (p 19) is controlled by phosphorylation. J. Biol. Chem. **272**, 8129–8132

6 Larsson, N., Marklund, U., Gradin, H. M., Brattsand, G. and Gullberg, M. (1997) Control of microtubule dynamics by oncoprotein 18: dissection of the regulatory role of multisite phosphorylation during mitosis. Mol. Cell. Biol. **17**, 5530–5539

7 Curmi, P., Maucuer, A., Asselin, S., Lecourtois, M., Chaffotte, A., Schmitter, J. M. and Sobel, A. (1994) Molecular characterization of human stathmin expressed in *Escherichia coli*: site-directed mutagenesis of two phosphorylatable serines (Ser-25 and Ser-63). Biochem. J. **300**, 331–338

8 Beretta, L., Boutterin, M. C. and Sobel, A. (1988) Phosphorylation of intracellular proteins related to the multihormonal regulation of prolactin: comparison of normal anterior pituitary cells in culture with the tumor-derived GH cell lines. Endocrinology **122**, 40–51

9 Doye, V., Boutterin, M. C. and Sobel, A. (1990) Phosphorylation of stathmin and other proteins related to nerve growth factor-induced regulation of PC12 cells. J. Biol. Chem. **265**, 11650–11655

10 Chneiweiss, H., Cordier, J. and Sobel, A. (1992) Stathmin phosphorylation is regulated in striatal neurons by vasoactive intestinal peptide and monoamines via multiple intracellular pathways. J. Neurochem. **58**, 282–289

11 Sobel, A. (1991) Stathmin: a relay phosphoprotein for multiple signal transduction? Trends Biochem. Sci. **16**, 301–305

12 Gavet, O., Ozon, S., Manceau, V., Lawler, S., Curmi, P. and Sobel, A. (1998) The stathmin phosphoprotein family. Intracellular localization and effects on the microtubule network. J. Cell Sci. **111**, 3333–3346

13 Holmfeldt, P., Larsson, N., Segerman, B., Howell, B., Morabito, J., Cassimeris, L. and Gullberg, M. (2001) The catastrophe-promoting activity of ectopic Op18/stathmin is required for disruption of mitotic spindles but not interphase microtubules. Mol. Biol. Cell **12**, 73–83

14 Melhem, R. F., Zhu, X. X., Hailat, N., Strahler, J. R. and Hanash, S. M. (1991) Characterization of the gene for a proliferation-related phosphoprotein (oncoprotein 18) expressed in high amounts in acute leukemia. J. Biol. Chem. **266**, 17747–17753

15 Brattsand, G. (2000) Correlation of oncoprotein 18/stathmin expression in human breast cancer with established prognostic factors. Br. J. Cancer **83**, 311–318

16 Curmi, P. A., Noguès, C., Lachkar, S., Carelle, N., Gonthier, M. P., Sobel, A., Lidereau, R. and Bièche, I. (2000) Overexpression of stathmin in breast carcinomas points out to highly proliferative tumours. Br. J. Cancer **82**, 142–150

17 Ghosh, P. K., Anderson, N. G., Cohen, P., Taketo, M., Atweh, G. F. and Lebowitz, P. (1993) Expression of the leukemia-associated gene p18 in normal and malignant tissues: inactivation of expression in a patient with cleaved B-cell lymphoma/leukemia. Oncogene **8**, 2869–2872

18 Jourdain, L., Curmi, P., Sobel, A., Pantaloni, D. and Carlier, M. F. (1997) Stathmin: a tubulin-sequestering protein which forms a ternary T2S complex with two tubulin molecules. Biochemistry **36**, 10817–10821

19 Curmi, P. A., Andersen, S. S. L., Lachkar, S., Gavet, O., Karsenti, E., Knossow, M. and Sobel, A. (1997) The stathmin/tubulin interaction *in vitro*. J. Biol. Chem. **272**, 25029–25036

20 Steinmetz, M. O., Kammerer, R. A., Jahnke, W., Goldie, K. N., Lustig, A. and van Oostrum, J. (2000) Op18/stathmin caps a kinked protofilament-like tubulin tetramer. EMBO J. **19**, 572–580

21 Gigant, B., Curmi, P. A., Martin-Barbey, C., Charbaut, E., Lachkar, S., Lebeau, L., Siavoshian, S., Sobel, A. and Knossow, M. (2000) The 4 Å X-ray structure of a tubulin:stathmin-like domain complex. Cell (Cambridge, Mass.) **102**, 809–816

22 Redeker, V., Lachkar, S., Siavoshian, S., Charbaut, E., Rossier, J., Sobel, A. and Curmi, P. (2000) Probing the native structure of stathmin and its interaction domains with tubulin. J. Biol. Chem. **275**, 6841–6849

23 Howell, B., Larsson, N., Gullberg, M. and Cassimeris, L. (1999) Dissociation of the tubulin-sequestering and microtubule catastrophe-promoting activities of oncoprotein 18/stathmin. Mol. Biol. Cell **10**, 105–118

24 Larsson, N., Segerman, B., Howell, B., Fridell, K., Cassimeris, L. and Gullberg, M. (1999) Op18/stathmin mediates multiple region-specific tubulin and microtubule-regulating activities. J. Cell Biol. **146**, 1289–1302

25 Stein, R., Mori, N., Matthews, K., Lo, L. C. and Anderson, D. J. (1988) The NGF-inducible SCG10 mRNA encodes a novel membrane-bound protein present in growth cones and abundant in developing neurons. Neuron **1**, 463–476

26 Ozon, S., Maucuer, A. and Sobel, A. (1997) The stathmin family: molecular and biological characterization of novel mammalian proteins expressed in the nervous system. Eur. J. Biochem. **248**, 794–806

27 Ozon, S., Byk, T. and Sobel, A. (1998) SCLIP: a novel SCG10-like protein of the stathmin family expressed in the nervous system. J. Neurochem. **70**, 2386–2396
28 Charbaut, E., Curmi, P. A., Ozon, S., Lachkar, S., Redeker, V. and Sobel, A. (2001) Stathmin family proteins display specific molecular and tubulin binding properties. J. Biol. Chem. **276**, 16146–16154
29 Maucuer, A., Doye, V. and Sobel, A. (1990) A single amino acid difference distinguishes the human and the rat sequences of stathmin, a ubiquitous intracellular phosphoprotein associated with cell regulations. FEBS Lett. **264**, 275–278
30 Muller, D. R., Schindler, P., Towbin, H., Wirth, U., Voshol, H., Hoving, S. and Steinmetz, M. O. (2001) Isotope-tagged cross-linking reagents. A new tool in mass spectrometric protein interaction analysis. Anal. Chem. **73**, 1927–1934
31 Sambrook, J., Fritsch, E. F. and Maniatis, T. (1989) Molecular Cloning: A Laboratory Manual, Cold Spring Harbor Laboratory Press, Cold Spring Harbor, NY
32 Tsao, K. L., DeBarbieri, B., Michel, H. and Waugh, D. S. (1996) A versatile plasmid expression vector for the production of biotinylated proteins by site-specific, enzymatic modification in *Escherichia coli*. Gene **169**, 59–64
33 Shelanski, M. L., Gaskin, F. and Cantor, C. R. (1973) Microtubule assembly in the absence of added nucleotides. Proc. Natl. Acad. Sci. U.S.A. **70**, 765–768
34 Weingarten, M. D., Lockwood, A. H., Hwo, S. Y. and Kirschner, M. W. (1975) A protein factor essential for microtubule assembly. Proc. Natl. Acad. Sci. U.S.A. **72**, 1858–1862
35 Detrich, III, H. W. and Williams, R. C. (1978) Reversible dissociation of the $\alpha\beta$ dimer of tubulin from bovine brain. Biochemistry **17**, 3900–3917
36 Carlier, M.-F. and Pantaloni, D. (1978) Kinetic analysis of cooperativity in tubulin polymerization in the presence of guanosine di- or triphosphate nucleotides. Biochemistry **17**, 1908–1915
37 Siegel, L. M. and Monty, K. J. (1966) Determination of the molecular weights and frictional ratios of proteins in impure systems by use of gel filtration and density gradient centrifugation. Application to crude preparations of sulfite and hydroxylamine reductases. Biochim. Biophys. Acta **112**, 346–362
38 Deleage, G. and Roux, B. (1987) An algorithm for protein secondary structure prediction based on class prediction. Protein Eng. **1**, 289–294
39 Sackett, D. L. (1997) Natural osmolyte trimethylamine *N*-oxide stimulates tubulin polymerization and reverses urea inhibition. Am. J. Physiol. **273**, R669–R676
40 Amayed, P., Pantaloni, D. and Carlier, M. F. (2002) The effect of stathmin phosphorylation on microtubule assembly depends on tubulin critical concentration. J. Biol. Chem. **277**, 22718–22724
41 Wallon, G., Rappsilber, J., Mann, M. and Serrano, L. (2000) Model for stathmin/OP18 binding to tubulin. EMBO J. **19**, 213–222
42 Steinmetz, M. O., Jahnke, W., Towbin, H., Garcia-Echeverria, C., Voshol, H., Muller, D. and van Oostrum, J. (2001) Phosphorylation disrupts the central helix in Op18/stathmin and suppresses binding to tubulin. EMBO Rep. **2**, 505–510
43 Di Paolo, G., Lutjens, R., Pellier, V., Stimpson, S. A., Beuchat, M. A., Catsicas, M. and Grenningloh, G. (1997) Targeting of SCG10 to the area of the Golgi complex is mediated by its NH_2-terminal region. J. Biol. Chem. **272**, 5175–5182

Received 16 September 2003/9 December 2003; accepted 11 December 2003
Published as BJ Immediate Publication 11 December 2003, DOI 10.1042/BJ20031413